AAPS PharmSciTech

Physicochemical Stability of Cimetidine Amorphous Forms Estimated by Isothermal Microcalorimetry

Submitted: April 24, 2002; Accepted: October 17, 2002

Makoto Otsuka[1], Fumie Kato[1]and Yoshihisa Matsuda[1]

[1]Department of Pharmaceutical Technology, Kobe Pharmaceutical University, 4-19-1 Motoyama-Kitamachi, Higashi-Nada, Kobe 658, Japan

ABSTRACT The effect of humidity on the physicochemical properties of amorphous forms of cimetidine was investigated using differential scanning calorimetry, isothermal microcalorimetry, and x-ray diffraction analysis. Amorphous forms were obtained by the melting (amorphous form M [AM]) and the cotton candy (amorphous form C [AC]) methods. Thermal behaviors of AM and AC with or without seed crystals were measured using an isothermal microcalorimeter under various conditions of relative humidity (RH) and temperature, respectively. The crystallization kinetics of amorphous solids was analyzed based on 10 kinds of solid-state reaction models. AM transformed into form A at 11% RH, 50°C but transformed into a mixture of form A and monohydrate at 51% and 75% RH at 25°C. The mean crystallization times (MCTs) of the heat flow curve of AM and AC at 11% RH, 50°C were 47.82 and 32.00 hours, respectively, but at 11% RH, 25°C both were more than 4320 hours. In contrast, AC transformed into form A under all storage conditions. The MCTs of AC at 51% and 75% RH were 29.61 and 11.81 hours, respectively; whereas the MCTs of AM were 46.79 and 15.52 hours, respectively. The crystallization of amorphous solids followed the three-dimensional growth of nuclei (Avrami equation) with an induction period (IP). The IP for AM at 11% RH, 50ºC was more than 2 times that for AC, but the difference in the crystal growth rate constant (CR) between AC and AM was within 10%. The IP for AM at 75% RH, 25ºC was reduced to only 10% of the IP at 51% RH with increasing humidity, but the CR did not change significantly. In contrast, the IP for AC was slightly reduced at 75% RH compared with 51% RH, but the CR was about 5 times greater. At 75% RH, 25ºC, the IP and CR of AM were about one-fourth the values of AC. This result suggests that the crystallization process consists of an initial stage during which the nuclei are formed and a final stage of growth.

Corresponding Author:
Makoto Otsuka
Department of Pharmaceutical Technology, Kobe Pharmaceutical University, 4-19-1 Motoyama-Kitamachi, Higashi-Nada, Kobe 658, Japan
Telephone: 0011-81-78-441-7531
Facsimile: 0011-81-78-441-7532
E-mail: m-otsuka@kobepharma-u.ac.jp

KEYWORDS: isothermal microcalorimetry, crystallization, amorphous, physicochemical stability, cimetidine.

INTRODUCTION The bioavailability of pharmaceutical preparations of insoluble bulk drugs depends on their physicochemical properties and rate of dissolution in the gastrointestinal tract [1-3]. To improve the dissolution of insoluble pharmaceuticals, the particle size is often reduced and/or the solubility increased by producing amorphous forms using various pharmaceutical techniques. An amorphous preparation is a useful dosage form to improve the dissolution behavior of pharmaceuticals, but it is chemically unstable and easily transformed into a stable form during preservation. Therefore, to obtain pharmaceutical preparations containing amorphous solids, it is necessary to evaluate physicochemical stability and to choose an appropriate formulation, then validate production processes.

To shorten the period of development, the chemical stability of pharmaceuticals was evaluated in accelerated storage conditions at high temperature and high relative humidity (RH) by high-performance liquid chromatographic method. Differential scanning calorimetry (DSC) and thermogravimetry are frequently used to evaluate the physicochemical stability of a pharmaceutical preparation under accelerated conditions. Long-term stability during preservation at room temperature is generally predicted based on the accelerated data by using the Arrhenius equation, because ordinary methods are not sensitive enough to detect small thermal differences. However, it is known that the crystalline transformation around ambient temperature is not always the same as at high temperature. Therefore, it is not easy to predict transformation at room temperature from data obtained at a high temperature.

Isothermal microcalorimetry (IMC) was developed for the chemical and pharmaceutical fields. The instrument has a high sensitivity (0.1 μW) and a smaller sample capacity (several grams). The sensitivity is more than 4 orders of magnitude higher than that of DSC. Since almost all chemical, physical, and biological processes are accompanied by small heat exchanges, IMC is an effective

method of investigating changes in the physicochemical properties of pharmaceutical preparations under ambient conditions. The physical stability of some excipients and drugs has been studied by IMC (eg, moisture content [4,5], mutarotation of lactose [6], surface energy [7], crystallization [8,9], and others [10-17]).

Cimetidine is a histamine H2 blocker, and there are several reports concerning the polymorphism of cimetidine [18,19]. Since the crystalline transformation induced bioavailability of pharmaceuticals, crystalline transformation of cimetidine was quantitatively investigated as a model drug. In this study, we obtained 2 kinds of amorphous forms of cimetidine and investigated both the stability during storage at various levels of humidity and the kinetic transformation leading to solid-state crystallization using IMC.

MATERIALS AND METHODS

Materials

Form A: A bulk powder of cimetidine of grade Japanese Pharmacopeia was obtained from Shanghai Bauzong Pharmaceutical Co Ltd. (Shanghai, China) Monohydrate: A hot 15% wt/wt aqueous solution of cimetidine was poured into a 5-fold excess of ice [18,19].

Amorphous form M (AM): The bulk powder was heated at 150°C and poured into liquid nitrogen. The mass was ground in an agate mortar and pestle.

Amorphous form C (AC): The bulk powder of cimetidine (500 mg) was compressed at 196 MPa by a compression/tension tester (Autograph, model IS-5000, Shimadzu Co, Kyoto, Japan) with an 8-mm punch and a die with flat surfaces at a speed of 25 mm/min. The pellets were ground in an agate mortar and sieved with 310 and 420 μm screens. A cotton candy machine was set up at about 150°C and rotated at 2600 rpm. The granules were put into the cotton candy machine (Cotton candy machine TK-5, Arahata Co, Shizuoka, Japan). The granules melted at 150°C while simultaneously extending because of centrifugal force, and then cooled down at room temperature.

Nuclear magnetic resonance spectroscopy

The proton nuclear magnetic resonance (NMR) spectra of an approximately 3% solution of the sample in fully deuterated acetone were recorded at 200 MHz (model XL-200; Varian, Palo Alto, CA). The proton NMR spectra of samples were compared with that of the bulk powder. No impurity was detected in the sample modifications.

X-ray powder diffraction analysis

X-ray powder diffraction profiles were taken with an x-ray diffractometer (XD-3A, Shimadzu Co). The measurement conditions were as follows: target, Cu; filter, Ni; voltage, 20 kV; current, 20 mA; receiving slit, 0.1 mm; time constant, 1 second; scanning speed 4°/2θ min.

Thermal analysis

DSC was performed with a type 3100 instrument (Mac Science Co, Tokyo, Japan). The operating conditions in an open-pan system were as follows: sample weight, 5 mg; heating rate, 10°C/min; N_2 gas flow rate, 30 mL/min. The monohydrate content of the samples was evaluated based on the heat of dehydration of an endothermic peak at 73ºC.

Isothermal microcalorimetric analysis

Isothermal behavior was measured using an isothermal microcalorimeter (Model 4400, Calorimetry Science Corp. Provo, USA), which consisted of a reference and 3 sample cells. The measurement chamber was a 40-mL glass vial containing two 2-mL glass tubes. One glass tube contained 100 mg of the sample, and the other contained saturated aqueous salt solutions (LiCl, $Ca(NO_3)_2 \cdot 4H_2O$, and NaCl saturated solutions were for 11% RH at 50°C, 51% RH at 25°C, and 75% RH at 25°C, respectively) to control the RH. The sample tube was sealed with a rubber cap. A glass sample vial, containing both the sample and saturated salt solution tubes and sealed with an aluminum cap, was placed into a preheating box for approximately 30 minutes. After prestorage, the rubber seal of the sample tube was pierced with a needle, and the measurement was started.

Scanning electron microscopy

The powder samples were coated with gold in an ion-sputter JFC-1100 (Jeol Datum Co, Tokyo, Japan), and photographs of samples were taken with a scanning electron microscope (model JSM-5200LV, Jeol Datum Co).

Isothermal kinetic analysis of the crystallization

The crystallization kinetics of amorphous solids was analyzed based on 10 kinds of solid-state reaction models, as shown in **Table 1** [20,21]. The kinetic equation of crystallinity involves a function f(x), and its integrated form is the function g(x) (x = 0.05-0.95), where x), is the function of crystallinity at time t.

Table 1. Kinetic Equations for the Most Common Mechanism of Solid-State Reactions

Symbol	g (*x*)	Mechanism
R_1	x	Zero-order mechanism (Polany-Winger equation)
R_2	$2[1 - (1 - x)]^{1/2}$	Two-dimensional phase-boundary mechanism
R_3	$3[1 - (1 - x)]^{1/3}$	Three-dimensional phase-boundary mechanism
F_1	$-\ln (1 - x)$	First-order mechanism
A_2	$[-\ln (1 - x)]^{1/2}$	Two-dimensional growth of nuclei mechanism (Avrami equation)
A_3	$[-\ln (1 - x)]^{1/3}$	Three-dimensional growth of nuclei mechanism (Avrami equation)
D_1	x^2	One-dimensional diffusion mechanism
D_2	$(1 - x) \ln (1 - x) + x$	Two-dimensional diffusion mechanism
D_3	$[1 - (1 - x)^{1/3}]^2$	Three-dimensional diffusion mechanism (Jander equation)
D_4	$(1 - 2x/3) - (1 - x)^{2/3}$	Three-dimensional diffusion mechanism (Ginstiling-Brounshtein equation)

RESULTS AND DISCUSSION

Physicochemical characterization of cimetidine polymorphs and amorphous forms

Figures 1 and **2** show the powder x-ray diffraction profiles and DSC profiles of form A (anhydrate), monohydrate, AM, and AC. The main x-ray diffraction peaks of form A were at 16.7°C, 17.8°C, 23.5°C, 26.0°C, and 27.2°C (2θ), while those of the monohydrate were at 13.8°C, 15.1°C, 15.8°C, 20.7°C, and 26.0°C (2θ). AM and AC showed no diffraction peak and a halo pattern, respectively. The DSC curves of form A had an endothermic peak at 143°C due to melting. The monohydrate had an endothermic peak at 73°C due to dehydration, an exothermic peak at 84°C to 95°C due to transformation into form A, and then an endothermic peak at 120°C to 130°C due to melting. AM had no thermo peak due to phase change. In contrast, AC had an endothermic peak at 55°C due to a phase transition to glass, transformed into a supercoolant solution, and then had an exothermic peak at 80°C to 110°C and an endothermic peak at 140°C due to crystallization and melting, respectively. These results indicated that both AM and AC were amorphous forms, with AM more kinetically stable than AC during the storage period. **Figure 3** shows scanning electron microscopy (SEM) photographs of form A, monohydrate, AM, and AC. Form A is a platelet crystal with a smooth surface. The monohydrate is an aggregated particle consisting of small cubic crystals. AM is a lump with a glossy surface, and AC is a fibrous-shape particle with a smooth surface.

Effect of humidity on the crystallization of AM and AC as determined by IMC

The effect of humidity on the crystallization of AM and AC was investigated by IMC. **Figure 4** shows the heat flow curves of AM and AC at various levels of humidity. After being stored at 11% RH, 25°C for over 6 months,

AM showed a halo pattern on the x-ray diffraction profile. This suggested that it did not transform into a crystalline form and was a stable amorphous form. In contrast, AC gradually transformed into a crystalline form at 25°C. AM and AC isothermal heat flow curves (**Figure 4a and 4d**) at 11% RH, 50°C showed broad peaks. The peak of AM and AC shifted on long-term storage with increasing RH, indicating that hydration of amorphous solid was accelerated by humidity. The peak of AC appeared earlier than that of AM under all RH and temperature conditions, suggesting that AM was kinetically more stable than AC.

To evaluate the physicochemical stability of amorphous solids, degree of crystallinity at time t was evaluated based on an exothermic peak area at time t on heat flow curve due to crystallization of AM or AC by IMC. The mean crystallization time (MCT) was calculated based on the degree of crystallinity versus time plot using the moment method [22] using a below equation. Results are summarized in **Table 2**.

$$MCT = \frac{\int_0^\infty t(\frac{dX}{dt})dt}{\int_0^\infty (\frac{dX}{dt})dt} = \frac{1}{X(\infty)}\int_0^\infty tdX$$

where *X* is amount of crystallized drug and *t* is time.

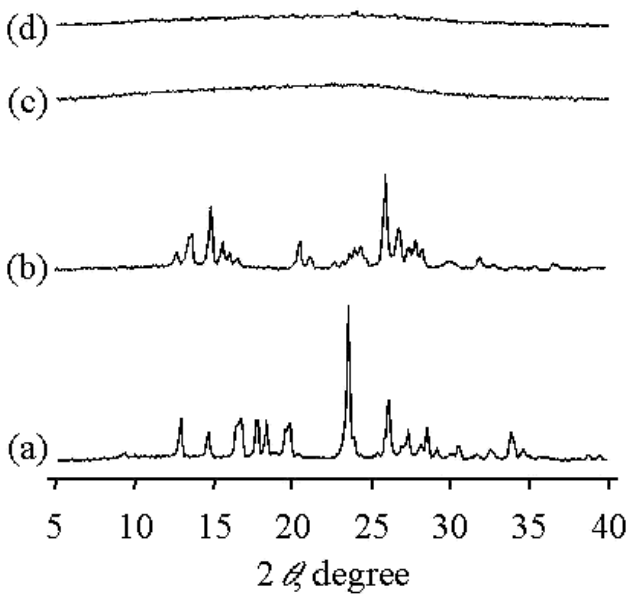

Figure 1. Powder x-ray diffraction profiles of cimetidine (a) form A; (b) monohydrate; (c) AM; (d) AC.

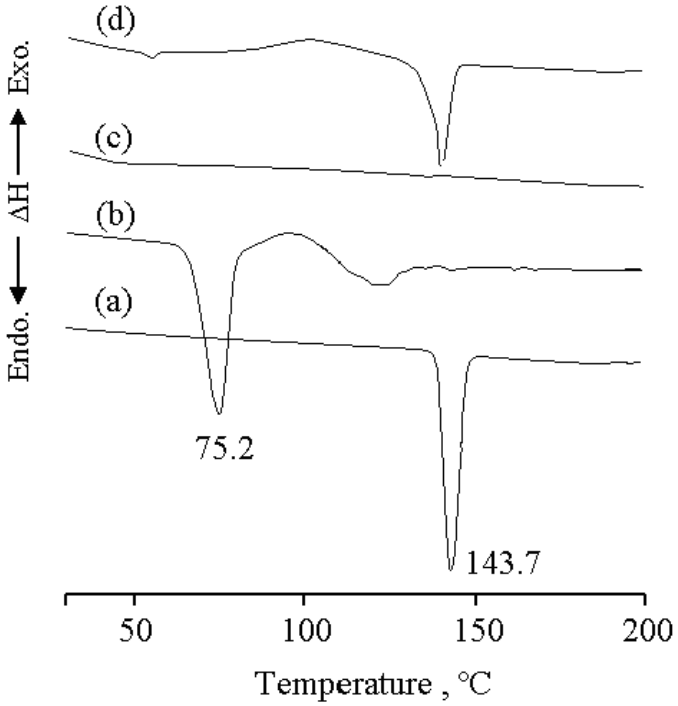

Figure 2. DSC thermograms of cimetidine (a) form A; (b) monohydrate; (c) AM; (d) AC.

The MCTs of the heat flow curve of AM and AC at 11% RH, 50°C were 47.82 and 32.00 hours, respectively, but the MCTs of both at 11% RH, 25°C were more than 4320 hours, indicating that the crystallization of AM and AC was accelerated at high temperature, and AM was more stable than AC at high temperature. On the other hand, the MCT of AC at 51% and 75% RH was 29.61 and 11.81 hours, respectively, whereas that of AM was 46.79 and 15.52 hours, respectively. The MCT of AC was shorter than that of AM at all RH conditions. This determination indicated that the crystallization of both amorphous solids was accelerated by humidity and that AM was more stable than AC at high humidity.

Effect of humidity on the crystallization kinetics of AM and AC

To clarify the kinetic mechanism of crystallization of amorphous cimetidine under isothermal conditions, the fraction of crystallization was evaluated based on the heat of crystallization of AM and AC (**Figure 4**), and kinetic parameters were calculated based on 10 kinds of solid-state kinetic equations as shown in **Table 1**. **Figure 5** shows plots of g(x) applied to the A3, R3, and D3 models against crystallization time. The linearity of the plots of the models was evaluated by the least-squares method, and the results are shown in **Table 3**. The best plot for the crystallization of amorphous cimetidine was with the three-dimensional growth of nuclei equation (Avrami equation) (A3). The mechanism was also supported by SEM observation of AM and AC transformed into aggregated plate-like crystals. This result indicated that the crystallization consisted of a nuclei formation process as an induction period (initial stage) and a growth process of nuclei (later stage).

Figures 6 and **7** show x-ray diffraction profiles and DSC curves of AM and AC after storage under various conditions of humidity, respectively. The x-ray diffraction and DSC results suggested that AC transformed into form A under all conditions, but AM transformed into mixtures of form A and monohydrate at 51% and 75% RH. After storage at 75% RH and 25ºC, AM contained 18.6% ± 6.5% monohydrate crystals as measured by the heat of dehydration at 73ºC, as shown in **Table 4**.

Figure 8 shows the surface view of AM and AC by SEM after crystallization under various storage conditions. This suggests that AM and AC were transformed into aggregated plate-like crystals. The shape of the transformed crystals of AM and AC also supported that the crystallization kinetics of those samples followed the A3 kinetics model.

The effects of humidity and temperature on the isothermal kinetic parameters of AM and AC are summarized in **Figure 9** and **Tables 5** and **6**. The induction period for AM at 11% RH, 50ºC was more than 2 times that for AC, but the difference in the crystal growth rate constant between AC and AM was within 10%. This indicated that

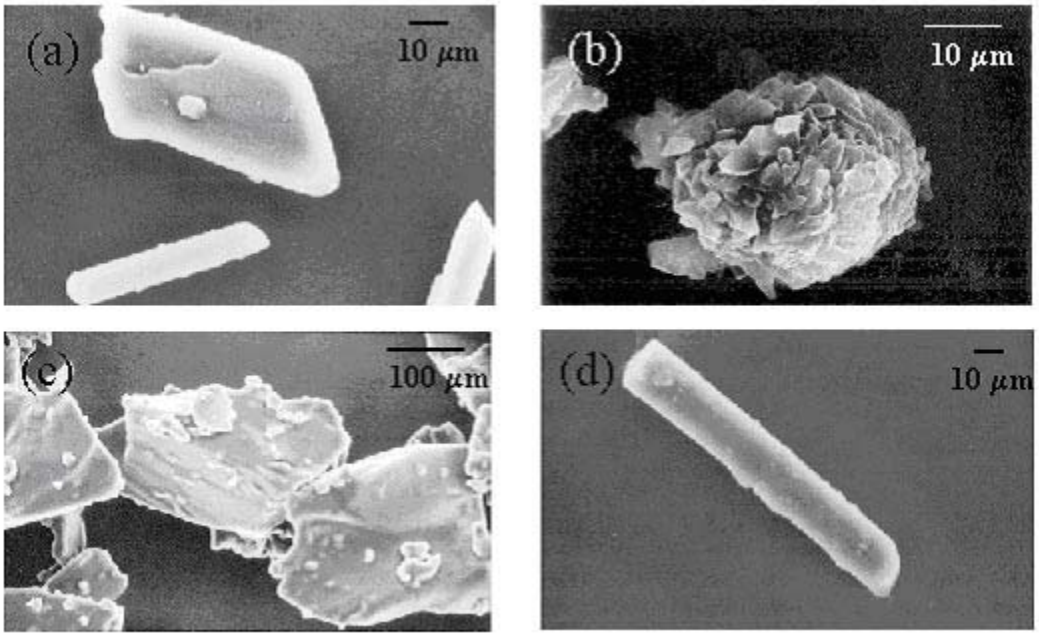

Figure 3. SEM photographs of cimetidine (a) form A; (b) monohydrate; (c) AM; (d) AC.

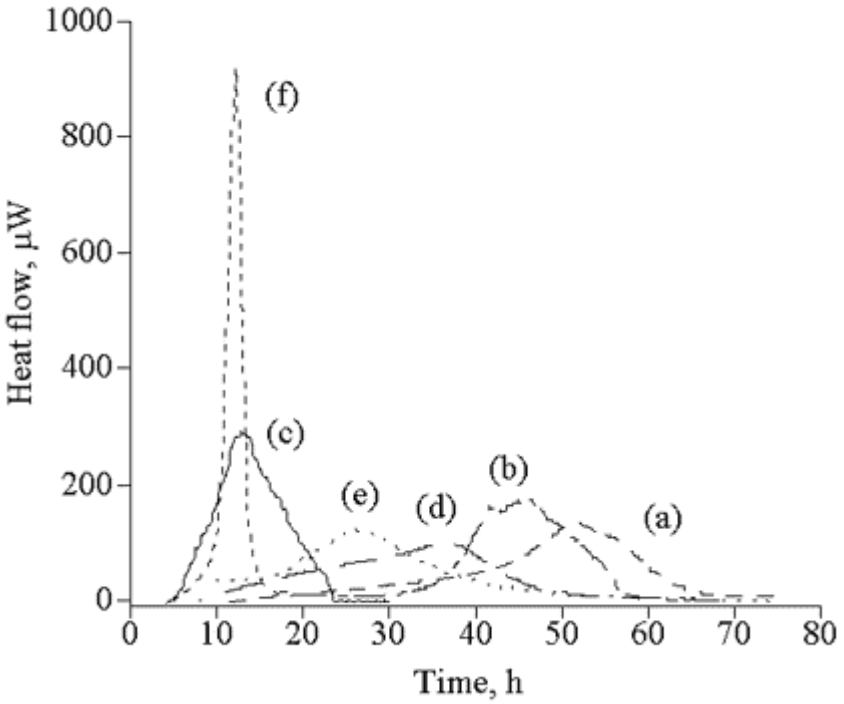

Figure 4. Heat flow curves of AM and AC obtained by isothermal calorimetry. AM: (a) 11% RH (50°C); (b) 51% RH (25°C); (c) 75% RH (25°C). AC: (d) 11% RH (50°C); (e) 51% RH (25°C); (f) 75% RH (25°C).

Table 2. Mean Crystallization Time of AM and AC Containing Crystalline Seeds*

	Mean Crystallization Time, h (S.D.)			
	25°C, 75% RH	25°C, 51% RH	25°C, 11% RH	50°C, 11% RH
AM	15.52 (1.02)	46.79 (1.78)	ND	47.82 (0.30)
AM + form A	11.04 (1.27)	34.17 (1.92)	-	30.06 (1.40)
AM + monohydrate	17.46 (1.52)	34.31 (0.43)	-	31.07 (0.14)
AC	11.81 (0.27)	29.61 (0.66)	ND	32.57 (0.88)
AC+ form A	9.49 (0.35)	19.47 (0.49)	-	31.00 (1.30)
AC + monohydrate	10.19 (0.22)	22.13 (0.24)	-	29.78 (1.35)

*AM indicates amorphous form M; AC, amorphous form C; RH, relative humidity; ND, not detected (n = 3).

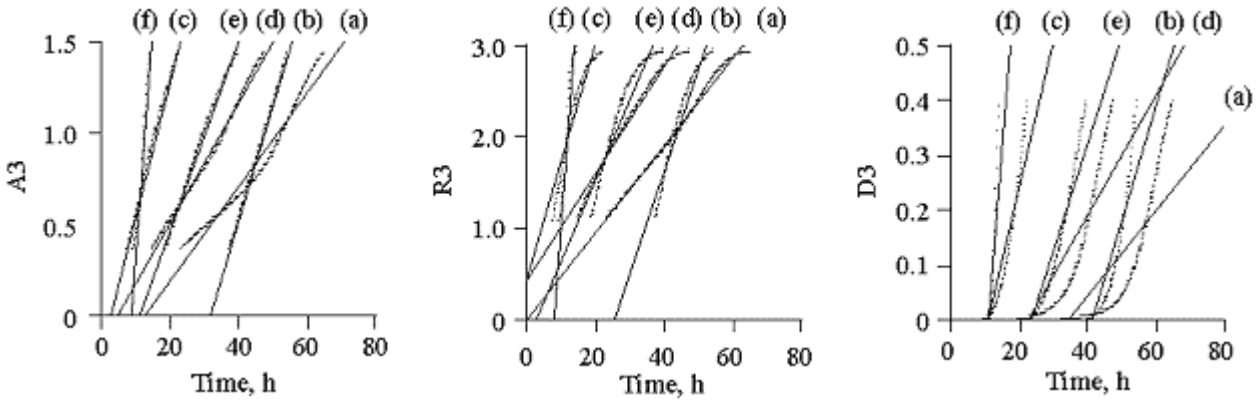

Figure 5. Dependence of the function g(x) on time for isothermal crystallization of AM. AM: (a) 11% RH (50°C); (b) 51% RH (25°C); (c) 75% RH (25°C). AC: (d) 11% RH (50°C); (e) 51% RH (25°C); (f) 75% RH (25°C). A3, R3, and D3 (see Table 1).

Table 3. Correlation Coefficients of Plots of g(x) Against Crystallization Time of AM and AC*

Model	AM			AC		
	75% RH	51% RH	11% RH	75% RH	51% RH	11% RH
A2	0.999	0.991	0.958	0.965	0.999	0.985
A3	0.997	0.998	0.978	0.980	0.996	0.996
R1	0.990	0.995	0.970	0.968	0.985	0.994
R2	0.969	0.992	0.994	0.987	0.965	0.996
R3	0.957	0.986	0.997	0.989	0.954	0.991
D1	0.988	0.961	0.902	0.942	0.987	0.953
D2	0.975	0.935	0.868	0.895	0.979	0.924
D3	0.938	0.883	0.813	0.853	0.952	0.873
D4	0.966	0.919	0.850	0.882	0.972	0.909

*AM indicates amorphous form M; AC, amorphous form C; RH, relative humidity.

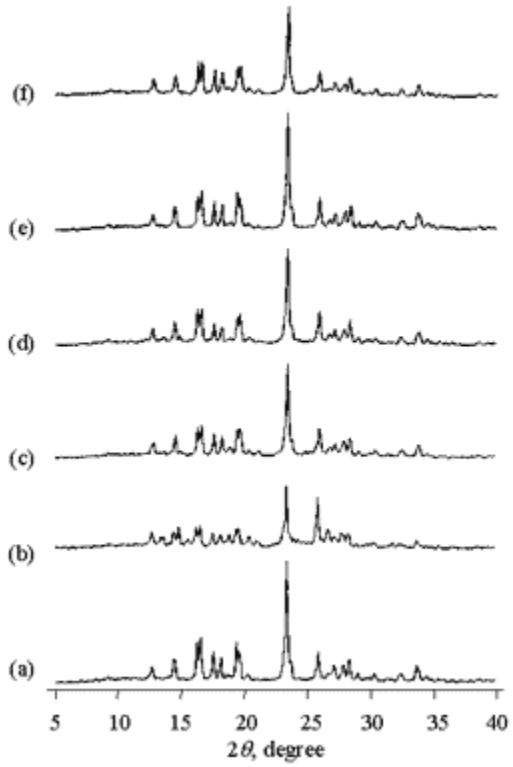

Figure 6. Powder x-ray diffraction profiles of AM and AC after crystallization in the microcalorimeter. (a) AM 11% RH (50°C); (b) AM 75% RH (25°C); (c) AC 11% RH; (d) AC 75% RH; (e) AM containing form A 75% RH; (f) AM containing monohydrate 75% RH.

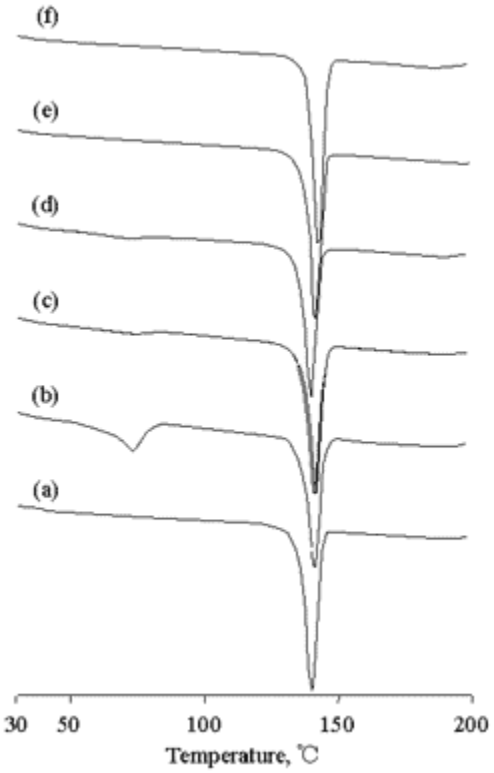

Figure 7. DSC thermograms of AM and AC after crystallization in the microcalorimeter. (a) AM 11% RH (50°C); (b) AM 75% RH (25°C); (c) AC 11% RH; (d) AC 75% RH; (e) AM containing form A 75% RH; (f) AM containing monohydrate 75% RH.

the difference in MCT was mainly due to the formation of nuclei, not crystal growth. The stability difference at low humidity might be related to drug diffusion attributable to the solid structure of the amorphous form.

The induction period for AM at 75% RH, 25ºC was reduced to only 10% of that at 51% RH with increasing humidity, but the crystallization rate constant did not change significantly. It was suggested that the critical nuclei formation of AM was accelerated by the increase in moisture, but this did not affect subsequent crystal growth. In contrast, the induction period for AC was slightly reduced at 75% RH compared with 51% RH, but the crystallization rate constant was about 5 times greater. This indicated that the crystal growth of AC was accelerated more than the nuclei formation by the increase in RH.

At 75% RH, 25ºC, the induction period and crystal growth rate constant of AM were about one fourth the values of AC. This indicated that the difference in MCT at high humidity between AC and AM was due to both the nuclei formation and crystal growth processes. According to these results, the stability difference at high humidity between AM and AC reflected that the solid-state structure was related to the formation of nuclei.

Effect of seed crystals on the isothermal kinetic behavior of cimetidine amorphous forms at various levels of humidity

To clarify the action of nuclei in the crystallization of amorphous solids, the thermal behavior of AM and AC containing 1% wt/wt form A or monohydrate as seed crystals was investigated by IMC.

Figure 10 shows heat flow curves of AM and AC containing 1% form A or monohydrate seed crystals at various levels of humidity. The MCT of AM decreased on addition of seed crystals as shown in **Table 2**, meaning that the crystallization was accelerated by the addition of both kinds of seed crystals. However form A was more effective in accelerating crystallization than monohydrate, as seed crystals. Since the main transformation of AM was to form A, it seems that form A was more effective in terms of crystallization than monohydrate. **Table 4** shows the monohydrate crystal content after isothermal microcalorimetric measurements of AM and AC contain

Table 4. Monohydrate Contents of AM and AC After Crystallization in the Isothermal Calorimeter*

	Monohydrate Content After Storage (SD)		
	75% RH	51% RH	11% RH
AM	18.59 (6.48)	9.52 (4.12)	0.00 (0.00)
AM + form A	0.00 (0.00)	0.00 (0.00)	0.00 (0.00)
AM + monohydrate	9.95 (3.30)	4.18 (1.80)	0.00 (0.00)
AC	0.00 (0.00)	0.00 (0.00)	0.00 (0.00)
AC+ form A	0.00 (0.00)	0.00 (0.00)	0.00 (0.00)
AC + monohydrate	0.00 (0.00)	0.00 (0.00)	0.00 (0.00)

*The monohydrate content of the samples of AC, AM + form A, AC + Form A, and AC + monohydrate was 0 after storage. The monohydrate contents were measured based on endothermic peaks of differential scanning calorimetry (DSC) curves (n = 3). AM indicates amorphous form M; AC, amorphous form C; RH, relative humidity.

Figure 8. SEM photographs of AM and AC after crystallization in the microcalorimeter. (a) AM 11% RH (50°C); (b) AM 75% RH (25°C); (c) AC 11% RH (50°C); (d) AC 75% RH (25°C).

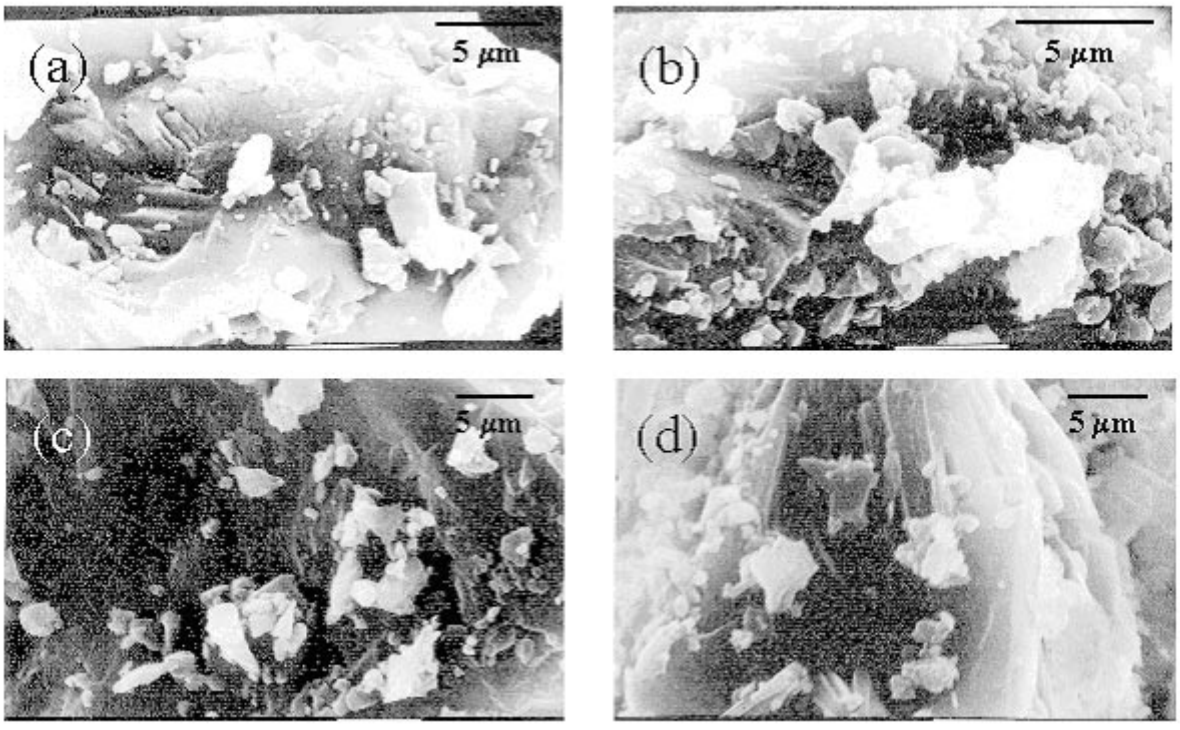

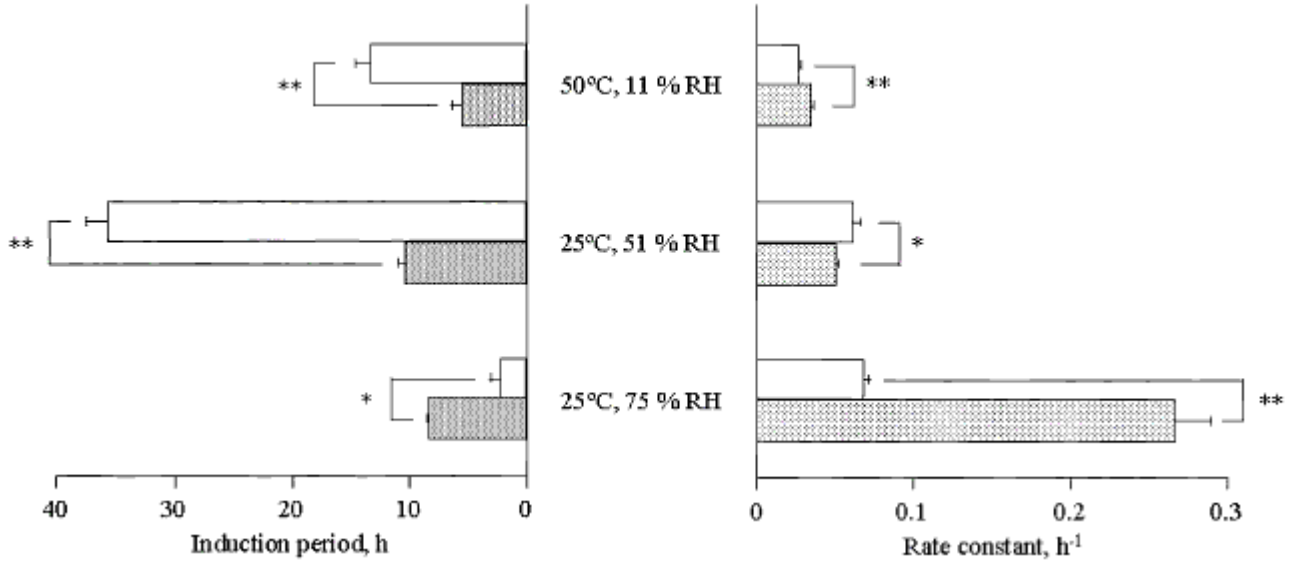

Figure 9. Kinetic parameters for crystallization of AM and AC by isothermal calorimetry. (a) induction period; (b) crystallization rate constant. Open bar is AM and closed bar is AC; *P < .05; **P < .005.

Table 5. Induction Period for Isothermal Crystallization of AM and AC Containing Crystalline Seeds*

	Induction Period, h (SD)			
	25°C, 75% RH	25°C, 51% RH	25°C, 11% RH	50°C, 11% RH
AM	1.97 (1.21)	35.48 (1.94)	ND	13.21 (1.40)
AM + form A	5.25 (1.12)	24.30 (1.49)	-	10.87 (4.46)
AM + monohydrate	3.63 (1.20)	24.41 (1.52)	-	10.13 (4.23)
AC	8.22 (0.05)	10.22 (0.75)	ND	5.28 (1.10)
AC+ form A	3.74 (0.85)	5.09 (0.24)	-	5.58 (1.79)
AC + monohydrate	4.59 (0.08)	8.78 (0.63)	-	5.31 (3.61)

*AM indicates amorphous form M; AC, amorphous form C; RH, relative humidity; ND, not detected (n = 3).

Table 6. Rate Constants for Isothermal Crystallization of AM and AC Containing Crystalline Seeds

	Crystallization Rate Constant, h^{-1} (S.D.)			
	25°C, 75% RH	25°C, 51% RH	25°C, 11% RH	50°C, 11% RH
AM	0.07 (0.01)	0.06 (0.01)	ND	0.03 (0.00)
AM + form A	0.16 (0.01)	0.09 (0.01)	-	0.05 (0.01)
AM + monohydrate	0.07 (0.01)	0.08 (0.00)	-	0.04 (0.01)
AC	0.27 (0.02)	0.05 (0.00)	ND	0.03 (0.00)
AC+ form A	0.16 (0.01)	0.06 (0.00)	-	0.03 (0.00)
AC + monohydrate	0.16 (0.01)	0.07 (0.00)	-	0.03 (0.01)

*AM indicates amorphous form M; AC, amorphous form C; RH, relative humidity; ND, not detected (n = 3).

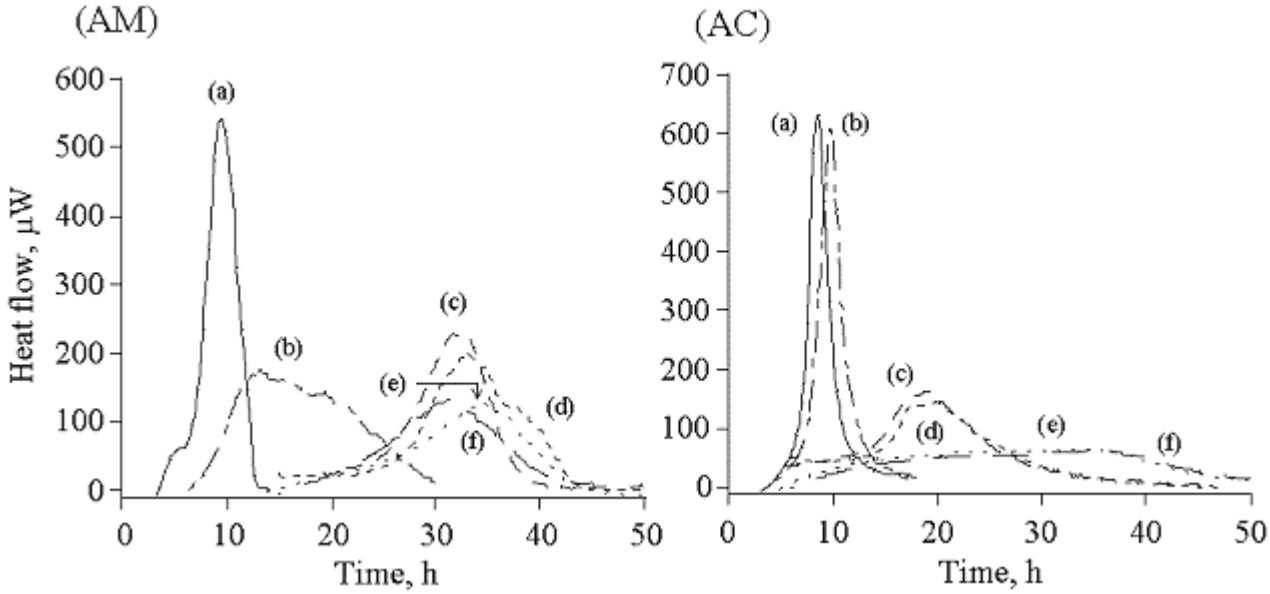

Figure 10. Heat flow curves of AM and AC containing crystalline seeds obtained by isothermal calorimetry. AM: (a) added form A at 75% RH (25°C); (b) added monohydrate at 75% RH (25°C); (c) added form A at 51% RH (25°C); (d) added monohydrate at 51% RH (25°C); (e) added form A at 11% RH (50°C); (f) added monohydrate at 11% RH (50°C). AC: (a) added form A at 75% RH (25°C); (b) added monohydrate at 75% RH (25°C); (c) added form A at 51% RH (25°C); (d) added monohydrate at 51% RH (25°C); (e) added form A at 11% RH (50°C); (f) added monohydrate at 11% RH (50°C).

ing 1% seed crystals. AM was transformed into form A under all storage conditions by adding form A seed crystals, but it was transformed into a mixture of form A and monohydrate by adding monohydrate seed crystals at 75% and 51% RH. In contrast, AC was transformed into form A by adding form A or monohydrate seed crystals under all conditions. **Tables 7** and **8** show the results of fitting crystallization kinetic models of AM and AC containing form A or monohydrate. The results and SEM indicated that AM and AC were transformed into stable solids following a three-dimensional growth of nuclei equation. In **Figure 11a**, at 75% RH the induction period for AM did not decrease on addition of seed crystals, while the crystallization rate constant increased on addi-

Table 7. Correlation Coefficients of Plots of g(x) Against Crystallization Time of AM Added to Form A or Monohydrate*

Model	AM + Form A			AM + Monohydrate		
	75% RH	51% RH	11% RH	75% RH	51% RH	11% RH
A2	0.969	0.983	0.972	0.997	0.991	0.982
A3	0.984	0.994	0.987	0.997	0.998	0.993
R1	0.975	0.989	0.982	0.990	0.994	0.986
R2	0.991	0.995	0.997	0.973	0.991	0.991
R3	0.993	0.993	0.997	0.962	0.984	0.988
D1	0.922	0.944	0.925	0.982	0.963	0.947
D2	0.893	0.916	0.894	0.968	0.937	0.945
D3	0.841	0.864	0.841	0.932	0.885	0.875
D4	0.877	0.900	0.877	0.958	0.922	0.907

*AM indicates amorphous form M; RH, relative humidity.

Table 8. Correlation Coefficients of Plots of g(x) Against Crystallization Time of AC Added to Form A or Monohydrate*

Model	AC + Form A			AC + Monohydrate		
	75% RH	51% RH	11% RH	75% RH	51% RH	11% RH
A2	0.984	0.996	0.997	0.989	0.998	0.998
A3	0.975	0.995	0.995	0.983	0.991	0.997
R1	0.954	0.983	0.985	0.964	0.978	0.988
R2	0.932	0.970	0.966	0.945	0.949	0.971
R3	0.921	0.961	0.954	0.935	0.934	0.960
D1	0.970	0.979	0.983	0.975	0.991	0.984
D2	0.978	0.970	0.976	0.979	0.988	0.974
D3	0.976	0.944	0.953	0.970	0.965	0.945
D4	0.980	0.964	0.969	0.978	0.983	0.966

*AC indicates amorphous form C; RH, relative humidity.

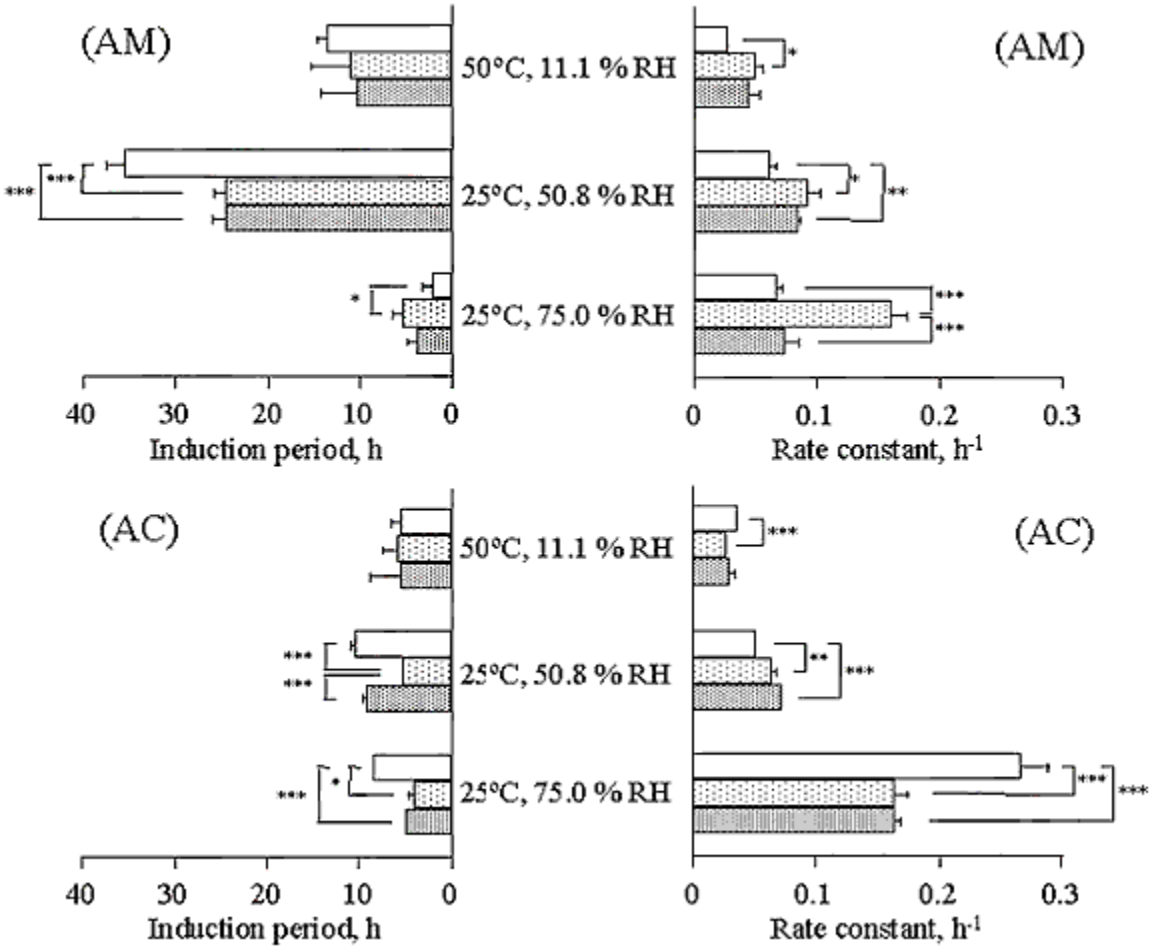

Figure 11. Kinetic parameters for crystallization of AM and AC containing crystalline seeds determined by isothermal calorimetry. Open bar is AM or AC; shadow bar is AM or AC containing form A; closed bar is AM or AC containing monohydrate. *P < .05; **P < .01; ***P < .005.

tion of form A, but not monohydrate. In contrast, the induction period and crystallization rate constant of AC decreased on addition of both form A and monohydrate.

At 51% RH the induction period for AM decreased on addition of both form A and monohydrate, and the crystallization rate increased. In contrast, the induction period for AC was decreased by addition of form A, and the crystallization rate constant increased by addition of form A and monohydrate: However the induction period for AC containing monohydrate crystalline seeds was not decreased.

At 50ºC, 11% RH, the induction period for AM and the crystallization rate constant of AC were unchanged, but the crystallization rate constant of AM increased on addition of form A.

These results suggest that AM transformed into form A at low humidity after the formation of form A as a crystal embryo, and into monohydrate at high humidity. In contrast, the induction period for AC was decreased by addition of both form A and monohydrate, but the crystallization constant changed little. Therefore, AM was more affected in terms of the growth of nuclei at high humidity than nuclei formation. It is considered that AC had a small amount of form A crystalline during the preparation and that this acted as a seed crystalline in the crystallization process. These crystalline transformations of metastable bulk powder might reduce solubility of the preparations and/or affect the disintegration time and dissolution rate of the products.

CONCLUSION

Two amorphous forms of cimetidine, AM and AC, were obtained by the melting and the cotton candy methods, and it was found that their solid-state stability at high RH and temperature differed significantly reflecting their solid structure. The stability of AM and AC was consistent with the physicochemical properties determined by

conventional x-ray diffractometry and DSC. Isothermal kinetics based on isothermal microcalorimetric data directly proved that crystallization of AM and AC proceeded based on the three-dimensional growth of nuclei. Therefore, it was indicated that nuclei formation and growth controlled their reactions, respectively. Since the results of isothermal kinetics were obtained at a relatively moderate storage temperature compared with the nonisothermal method (DSC), it might be possible to predict crystalline transformation rates at room temperature using the Arrhenius equation.

REFERENCES

1. Food and Drug Administration. Guidelines: manufacturing and controls for INDs and NDAs. Quoted by:Pharm Tech Japan. 1985;1:835-850.

2. Haleblian JK. Characterization of habits and crystalline modification of solids and their pharmaceutical applications. J Pharm Sci. 1975;64:1269-1288.

3. Otsuka M, Matsuda Y. Polymorphism, pharmaceutical aspects. In: Swarbrick J, Boylan JC, eds. Encyclopedia of Pharmaceutical Technology. Vol 12. New York, NY: Marcel Dekker; 1995:305-326.

4. Briggner L, Buckton G, Bystrom K, Darcy P. The use of isothermal microcalorimetry in the study of changes in crystallinity induced during the processing of powders. Int J Pharm. 1994;105:125-135.

5. Sebhatu T, Angberg M, Ahlneck C. Assessment of the degree of disorder in crystalline solids by isothermal microcalorimetry. Int J Pharm. 1994;104:135-144.

6. Angberg M, Nyström C, Castensson S. Evaluation of heat-conduction microcalorimetry in pharmaceutical stability studies, V: a new approach for continuous measurements in abundant water vapour. Int J Pharm. 1992;81:153-167.

7. Sheridan PL, Buckton G, Storey DE. Development of a flow microcalorimetry method for the assessment of surface properties of powders. Pharm Res. 1995;12:1025-1030.

8. Buckton G, Darcy P, Greenleaf D, Holbrook P. The use of isothermal microcalorimetry in the study of changes in crystallinity of spray-dried salbutamol sulphate. Int J Pharm. 1995;116:113-118.

9. Aso Y, Yoshioka S, Otsuka T, Kojima S. The physical stability of amorphous nifedipine determined by isothermal microcalorimetry. Chem Pharm Bull. 1995;43:300-303.

10. Rat M, Guillaume P, Wilker S, Pantel G. Practical application of microcalorimetry to the stability of propellants. Workshop Microcalorim Energ Mater. Defence Research Agency: Sevenoaks, UK. 1997;V1-V18.

11. Mimura H, Kitamura S, Koda S. Evaluation of drug stability by isothermal microcalorimetry. Netsu Sokutei. 1998;25(4):92-96.

12. Giron D. Thermal analysis, microcalorimetry and combined techniques for the study of pharmaceuticals. J Therm Anal Calorim. 1999;56(3):1285-1304.

13. Du W, Li X, Wang B, Zhang Y. A study on the interaction between cisplatin and urease. Thermochim Acta. 1999;333(2):109-114.

14. Beezer A, Gaisford S, Hills AK, Mitchell JC. Pharmaceutical microcalorimetry: applications to long-term stability studies. Int J Pharm. 1999;179(2):159-165.

15. Runge FE, Heger R. Use of microcalorimetry in monitoring stability. Example: vitamin A esters. J Agric Food Chem. 2000;48(1):47-55.

16. Tompa AS Jr, Bryant WF. Microcalorimetry and DSC study of the compatibility of energetic materials. Proc Workshop Microcalorim Energ Mater 2nd. Defence Research Agency: Sevenoaks, UK. 1999;Q1-Q21.

17. Phipps MA, Mackin LA. Application of isothermal calorimetry in solid state drug development. Pharm Sci Technol Today. 2000;3(1):9-17.

18. Shibata M, Kokubo H, Morimoto K, Morisaka K, Ishida T, Inoue M. X-ray structural studies and physicochemical properties of cimetidine polymorphism. J Pharm Sci. 1983;72:1436-1442.

19. Hegedüs B, Görög S. The polymorphism of cimetidine. J Pharm Biomed Anal. 1985;3:303-313.

20. Hancock JD, Sharp JH. Method of comparing solid-state kinetic data and its application to the decomposition of kaolinite, brucite, and BaCO3. J Am Ceram Soc. 1972;55:74-77.

21. Otsuka M, Kaneniwa N. Dehydration of cephalexin hydrates. Chem Pharm Bull. 1983;31:1021-1029.

22. Tanigawara Y, Yamakoka K, Nakagawa T, Uno T. Moment analysis for the separation of mean in vivo disintegration, dissolution, absorption, and disposition time of ampicillin products. J Pharm Sci. 1982;71(10):1129-1133.